Zircon U-Pb ages of the pegmatites in the Kontum massif, central Vietnam and their quality evaluation for ceramic industry

Truong Chi CUONG*,**, Pham Trung HIEU*,**, Pham MINH*,**, Kenta KAWAGUCHI***,†, Nong Thi Quynh ANH*,** and Khuong The HUNG‡

*Faculty of Geology, University of Science, Ho Chi Minh City, Vietnam
**Vietnam National University, Ho Chi Minh City, Vietnam
***Department of Earth and Environmental Sciences, Jeonbuk National University, Jeonju 54896, Republic of Korea
†Department of Earth and Planetary Systems Science, Graduate School of Science, Hiroshima University, Higashi-Hiroshima 739-8526, Japan
‡Faculty of Geosciences and Geoengineering, Hanoi University of Mining and Geology, Hanoi, Vietnam

Pegmatites occur in the Kontum massif as NE-SW oriented large dykes ranging from a few meters to several tens of meters in width. They consist of 3 stages of formation based on the difference of petrographic characteristics and ages: the first-stage pegmatites are characterized by quartz (40-45 vol%) and K-feldspar (55-60 vol%), the second-stage pegmatites are composed of K-feldspar (70 vol%), quartz (25 vol%), muscovite (<5 vol%), and biotite (<5 vol%), and the third-stage pegmatites are characterized by K-feldspar (60 vol%) and quartz (25 vol%). K-feldspar has common grain sizes of 0.5-1.0 cm with milky white color and shows perthitic texture. The emplacement ages of pegmatites determined by the zircon LA-ICP-MS U-Pb method yielded weighted mean $^{206}Pb/^{238}U$ ages of 448.2 ± 6.4 Ma (the first-stage), 269.4 ± 3.2 Ma (the second-stage), and 239 ± 3 Ma (the third-stage). The first-stage pegmatites coincide with the Ordovician-Silurian magmatism probably associated with the closure of an ancient oceanic basin within the Kontum massif. The second- and third-stage pegmatites can be linked with Permian-Triassic collisional magmatic activities. Host granitoids were also collected for petrographic investigations and age dating. Biotite-granite (Ben Giang-Que Son Complex) hosting the first- and second-stage pegmatites showed a magmatic age of 236.9 ± 2.9 Ma. Granites of the Van Canh Complex hosting the third-stage pegmatites yielded a similar age range between 244.2 ± 3.2 and 241.6 ± 1.7 Ma indicating that the third-stage pegmatite intruded shortly after the formation of the host granite. Based on quality assessments, samples from the second-stage pegmatites (~ 269 Ma) in the study area have the most applicable quality for ceramic manufacture and the technological samples fulfill Vietnam's ceramic standards (VN 6598:2000 standards).

Keywords: Kontum massif, Pegmatite, Zircon U-Pb dating, Ceramic

INTRODUCTION

Pegmatites are characterized by the occurrence of coarse-grained minerals such as quartz, feldspar, mica, and minor accessory minerals. Such pegmatites are considered to be potentially generated from magmatic melts during the late stage of the crystallization processes of massive batholiths. The plutonic magmas generating pegmatites are usually observed as large bodies spatially connecting roofward with smaller-scaled dike swarms of pegmatite segregations and are most commonly composed of granites (London, 2021). Normally, pegmatites can be formed under a wide range of temperature (200-700 °C), depth (1.5-20 km), and pressure (100-800 MPa) during the final magma process as a highly fractionated product (Burnham and Nekvasil, 1986). There have been many detailed studies on the origin of pegmatite all over the world (Moore, 1971; Wang et al., 2007; Liu et al., 2010), while others have dealt with the association of pegmatites and rare metal minerals (Gramaccioli and Segalstad, 1978; Veksler and Thomas, 2002; Mao et al., 2003). Pegmatites are commonly accompanied by metals, non-metals, and gem-quality minerals. Therefore, comprehensive studies on pegmatite have both scientific and industrial significance, particularly for economic geology. In Vietnam,

doi:10.2465/jmps.210911
K. Kawaguchi, kentakawaguchi2@gmail.com Corresponding author

numerous pegmatitic bodies have been outlined in geological mappings at different scales (e.g., 1:200000 and 1:50000) and attributed to the late magmatic stages. They are intruded into the basement comprising metamorphic rocks including metacarbonate formations as evidenced by their cross-cutting boundaries with hosting formations and foliation of the metamorphic basement (Thục and Trung, 1995; Toát, 2003). Pegmatitic rocks in the Kontum massif, central Vietnam have been well described in geological maps for their value on applied material research (e.g., Toát, 2003). Those studies mainly focused on the potential application of pegmatites in the ceramic industry from a few representative pegmatite bodies, while the origin, age, and mechanism of pegmatite formation have not been fully documented in any of those works. Therefore, investigations on the emplacement age of pegmatitic rock in the study area of central Vietnam will provide new and quantitative data to clarify the geological evolution in the Kontum massif. This study for the first time reports the zircon U-Pb ages of the pegmatitic rocks in the Kontum massif. Based on temporal correlation and genetic relationship between magmas and associated pegmatites, the premise of searching for coarse-grained K-feldspar minerals used in ceramics materials will be further facilitated.

GEOLOGICAL FRAMEWORK AND PETROGRAPHY

The Indochina block comprises three major geotectonic zones in the territory of Vietnam from north to south: the Truong Son belt, the Kontum massif, and the Dalat zone (Fig. 1; Tri and Khuc, 2011). The Kontum massif, central Vietnam is situated at the central-east part of the Indochina block bounded by the Dalat zone to the south and the Truong Son belt to the north (Fig. 1). Recent studies suggested that the Kontum massif has a long evolutionary history from Precambrian and had undergone multiple geological processes such as subduction-related arc setting and continental collision events causing metamorphism up to amphibolite- to granulite-facies conditions (Osanai et al., 2004; Nakano et al., 2007, 2013). Previous studies revealed that the Kontum massif recorded two significant magmatic-metamorphic activities: Ordovician-Silurian period (e.g., Carter et al., 2001; Nagy et al., 2001; Shi et al., 2015; Hieu et al., 2016; Nguyen et al., 2019; Jiang et al., 2020; Minh et al., 2020) and Permian-Triassic period (e.g., Sang, 2011; Hieu et al., 2015; Shi et al., 2015; Faure et al., 2018). Evidence of Archean magmatic activities in the Kontum massif has not been found, instead, Mesoproterozoic magmatic ages overprinted by the Triassic metamorphism have been reported from the Kontum massif (Nakano et al., 2021). Precambrian metamorphic complexes and Paleozoic, Mesozoic, and Cenozoic sedimentary formations are well exposed in the study area (Figs. 2b and 2c).

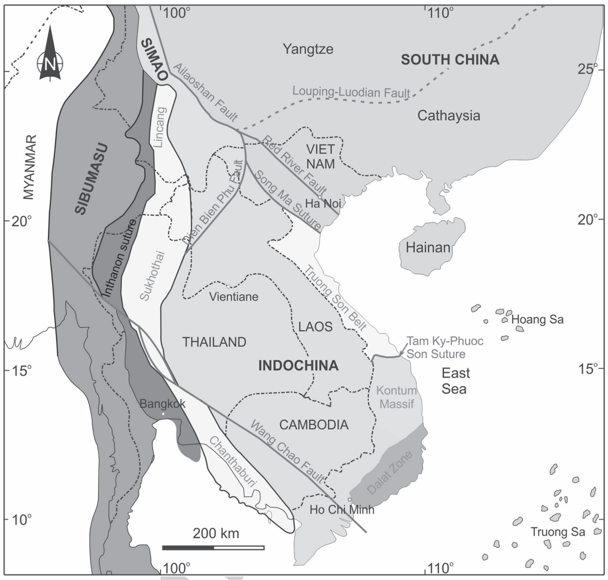

Figure 1. Geological map of SE Asia modified after Hieu et al. (2015). Color version is available online from https://doi.org/10.2465/jmps.210911.

Pegmatite bodies are widespread in the Kontum massif, comprising large dykes from a few meters to hundreds of meters, and oriented mostly in the NE-SW direction. In this study, we focus on two areas of the Kontum massif, viz., Dak Rve-Kon Go area (Kon Ray District, Kon Tum Province) (Fig. 2b) and To Tung area (K Bang District, Gia Lai Province) (Fig. 2c) where the pegmatite bodies have been reported (Tinh et al., 1997; Geological map Mang Den-Bong Son sheet).

In the Dak Rve-Kon Go area, first- and second-stage pegmatites penetrate the Paleoproterozoic metamorphic formations and felsic to intermediate plutons of the Ben Giang-Que Son Complex of I-type affinity (Fig. 2b; Sang, 2011). Two different zircon U-Pb ages of 479 ± 3 Ma (Hieu and Trung, 2015) and ~ 306-278 Ma (Sang, 2011) have been reported for the granitoids of the Ben Giang-Que Son Complex found in the Truong Son Belt. Hai Van Complex is mainly composed of S-type two-mica granite and shows the zircon U-Pb age of ~ 242-224 Ma (Hieu et al., 2015). Previous studies have proposed that the pegmatites in the study area were formed during a dyke intrusion phase genetically related to the Ben Giang-Que Son Complex or the Hai Van Complex (Toát, 2003). The pegmatites in Dak Rve-Kon Go area (Fig. 2b) show massive structures and medium to coarse grains, accompanied by sporadic quartz veins in several outcrops. In the field, pegmatites are characterized by K-feldspar with quartz and subordinate muscovite. Two-mica granites of the Hai

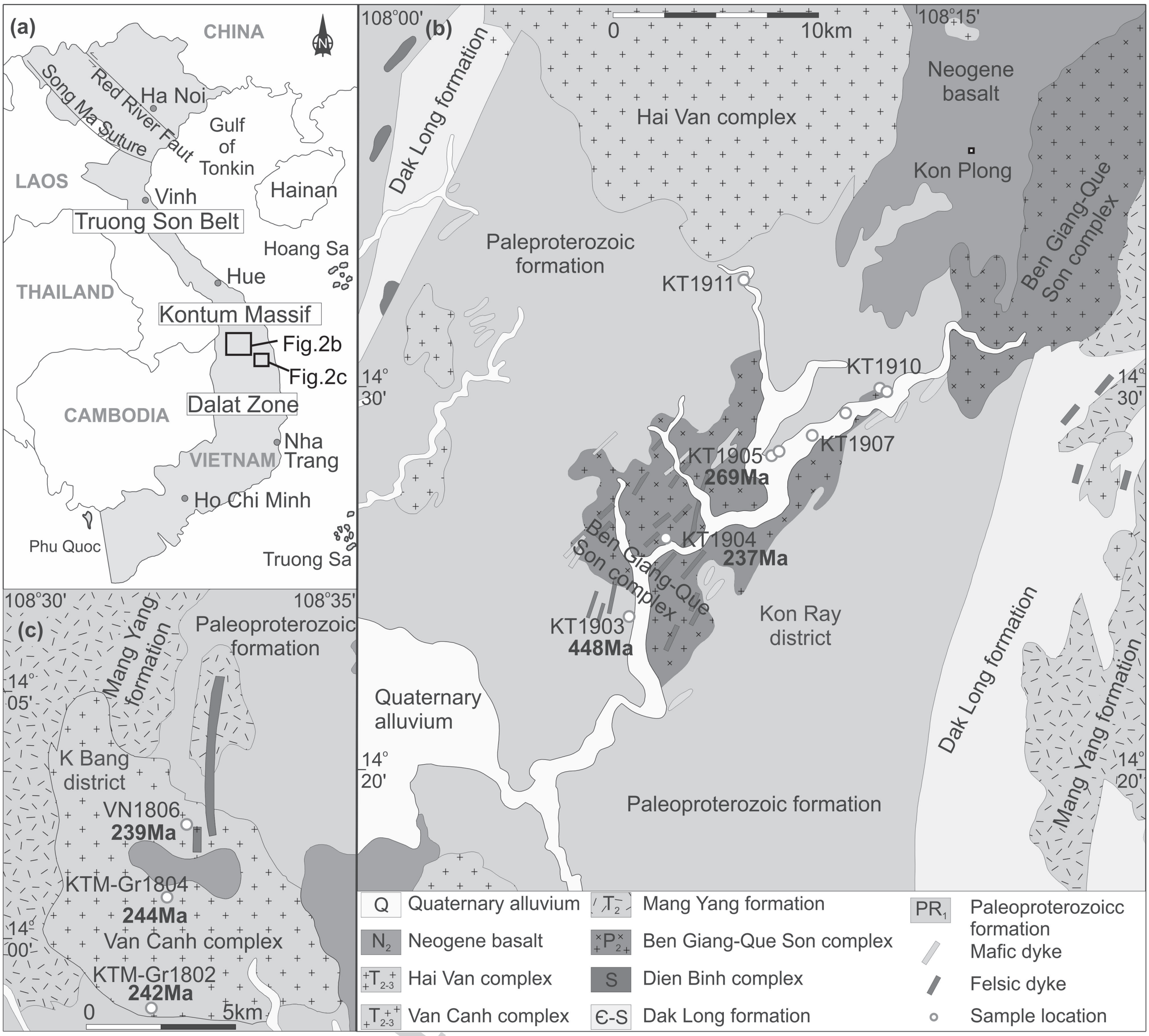

Figure 2. Simplified geological map including the occurrence of the pegmatites in the study area modified after Bao (2000). Color version is available online from https://doi.org/10.2465/jmps.210911.

Van Complex widely occur and the cross-cutting boundary between Hai Van granites and the Permian intrusions of Ben Giang-Que Son Complex is observed in some places (Tri and Khuc, 2011). Neogene basalts partly cover the magmatic-metamorphic complexes (Fig. 2b).

In the To Tung area, the Van Canh felsic-dominant plutonic complex is intruded into the Paleoproterozoic formation and the Mang Yang Formation (Fig. 2c). The magmatic age of the Van Canh granite was determined at ~ 251-229 Ma using the zircon U-Pb dating method (Hung et al., 2021; Tinh et al., 2021). The third-stage pegmatites are less widespread compared to the first- and second-stage pegmatites in the Dak Rve-Kon Go area, however, they show large dykes ranging from a few meters to hundreds of meters in width oriented in the N-S direction (Fig. 2c). Pegmatites penetrate the granitic intrusions of the Van Canh Complex and are unconformably overlain by Neogene basalts (Fig. 2c).

SAMPLE DESCRIPTION AND PETROGRAPHY

Outcrop and petrographic details of pegmatites and granites of the Dak Rye-Kon Go area

The first-stage pegmatite bodies from which the sample KT1903 was collected are NE-SW trending dykes with a moderate size of 5 m wide and 20-50 m long. Based on field observations, pegmatites penetrate mica-sillimanitequartz schists of Paleoproterozoic formation (Fig. 3c). Pegmatites are grayish-white and composed mainly of quartz (55-60 vol%) and K-feldspar (40-45 vol%) (Fig. 3e). The second-stage pegmatites (sample KT1905) appear to be the most widespread group in the study area; they are well-exposed throughout the Kon Ray District and are genetically related to the Ben Giang-Que Son Complex. With a common size of 8-14 m in width and 50-60 m in length, they extend in the NE-SW direction and penetrate granites of the Ben Giang-Que Son intrusive body (Figs. 3a and 3b). Pegmatites of this stage have a gray-white color. The major minerals include K-feldspar (~ 70 vol%) and quartz (~ 25 vol%), and minor minerals are muscovite, biotite, garnet, and sphene (Figs. 3f and 3g). K-feldspars are noticeably coarse-grained up to 1-2 cm and have milky white color and perthitic structure (Fig. 3g). Plagioclase grains show a typical albite twinning and occasionally a concentric zoning structure. The intergrowth of quartz and K-feldspar in the granophyric texture is commonly observed in most of the samples. Small-sized muscovite grains are found interspersed with K-feldspar (Fig. 3g). Two-mica granite from the Ben Giang-Que Son Complex (sample KT1904) is mainly composed of K-feldspar (30 vol%), plagioclase (30 vol%), quartz (30 vol%), biotite (5-6 vol%), and muscovite (3 vol%). Minor minerals (~ 1 vol%) include apatite, zircon, and ilmenite.

The first-stage pegmatite (sample KT1903), second-stage pegmatite (sample KT1905), and two-mica granite of the Ben Giang-Que Son Complex (sample KT1904) from this area were selected for the zircon U-Pb age dating (Fig. 2b). Four pegmatite samples of the second-stage (KT1907, KT1908, KT1909, and KT1910) were selected for the whole-rock major element analysis. Four pegmatite samples from the second-stage (KT1905, KT1907, KT1909, and KT1910) were chosen for the quality evaluation as raw materials for ceramic material (Fig. 2b).

Outcrop and petrographic details of pegmatites and granites of the To Tung area

The main rock-forming minerals in the biotite granite from the Van Canh Complex (sample KTM-Gr1802) are plagioclase (40 vol%), quartz (20 vol%), biotite (20 vol%), and K-feldspar (10 vol%) with minor clay minerals (<10 vol%). Common accessory phases are zircon, apatite, and opaque minerals. Two-mica granite of the Van Canh Complex (sample KTM-Gr1804) shows a mineral assemblage of quartz (30 vol%), K-feldspar (30 vol%), plagioclase (30 vol%), and biotite (5 vol%), with minor muscovite, zircon, apatite, and opaque minerals. The third-stage pegmatite (sample VN1806) composed mainly of K-feldspar (60 vol%) and quartz (25 vol%) is an N-S oriented dyke intruded into host granites of the Van Canh Complex (Fig. 3d).

The third-stage pegmatite (sample VN1806) and two Van Canh Complex samples [biotite granite (KTM-Gr1802) and two-mica granite (KTM-Gr1804)] from this area were selected for zircon U-Pb age dating (Fig. 2c). In addition, the third-stage pegmatite (sample VN1806) was selected for the whole-rock major element analysis and the quality evaluation as raw materials for ceramic material (Fig. 2c).

ANALYTICAL METHODS

Whole-rock geochemical analysis (Major elements)

Representative pegmatite samples of 0.2 kg were crushed and ground into a fine powder with a grain size of <0.01 mm using a vibration agate mill. Whole-rock powdered samples are ignited at 950 °C for one hour to determine loss on ignition (LOI). Major element concentrations were determined by powder pellet method using X-ray fluorescence spectrometry at the State Key Laboratory of Geological Process and Mineral Resources in Hanoi University of Mining and Geology, Vietnam. Analytical uncertainty is less than 5% for major elements.

LA-ICP-MS zircon U-Pb dating

Zircon grains from three pegmatites and three granites were separated from the crushed samples by panning methods. Zircon grains with few fractures were randomly handpicked under a binocular microscope. Picked zircon grains were mounted in epoxy resin together with the primary standard zircon FC1 (TIMS $^{207}Pb/^{206}Pb$ age of 1099.0 ± 0.6 Ma; Paces and Miller Jr, 1993) and secondary standard zircon YO1 (TIMS $^{206}Pb/^{238}U$ age of 279.3 Ma; Herzig et al., 1997) and polished to expose the interior of grains. To investigate the morphological and internal characteristics and to determine spot positions for U-Pb dating, zircon grains were studied using transmitted and reflected light microscopes and cathodoluminescence (CL) images obtained using a scanning electron microscope (SEM: JEOL JSM 7500F) installed at the Department of Earth and Planetary Systems Science, Hiroshima University, Japan. Zircon U-Pb isotope analysis was performed using a 213 nm Nd-YAG Laser (New Wave Research UP-213) attached with an inductively coupled plasma mass spectrometer (Thermo Fisher X-Series-II) (LA-ICP-MS) installed at the same department. Primary standard zircon FC1 was used to correct the U-Pb ratio, glass standard NIST SRM 610 was used to correct the Th/U ratio, and secondary standard zircon YO1 was

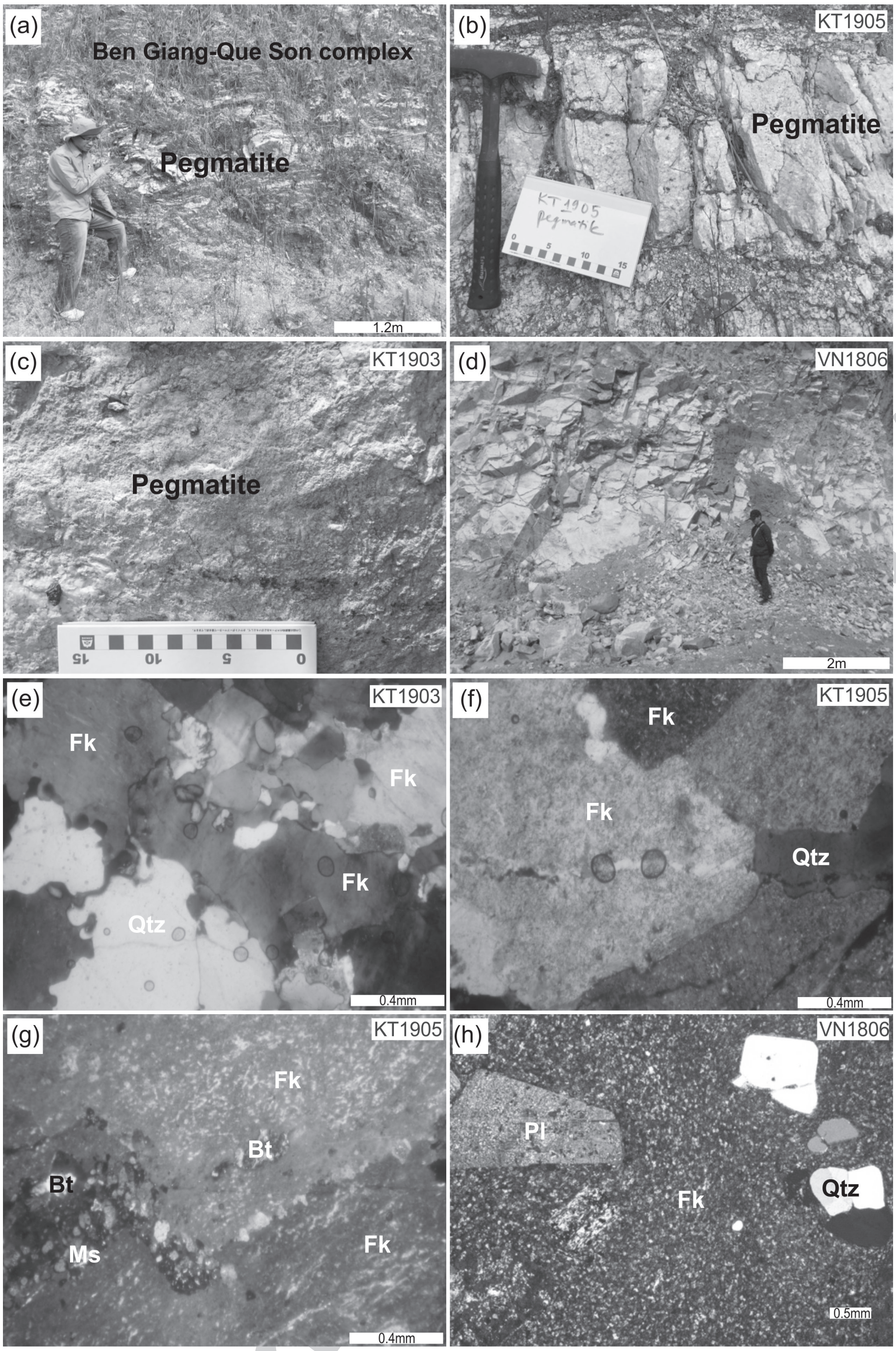

Figure 3. Outcrop and thin-section photographs of the pegmatite. Photomicrographs were obtained under a polarized light microscope. Pl, plagioclase; Bt, biotite; Ms, muscovite; Qtz, quartz and Fk, K-feldspar. Color version is available online from https://doi.org/10.2465/jmps.210911.

applied to evaluate measurement accuracy. During the analytical session, the weighted mean $^{206}Pb/^{238}U$ age of secondary standard zircon YO1 was 278.1 ± 3.3 Ma (MSWD = 0.25, n = 8), which is consistent with the recommended value. The laser spot size and repetition rate were maintained at 25 µm and 4 Hz, respectively. The weighted mean age is quoted at 95% confidence level, and the dates and isotopic ratios are at 2σ confidence level. Data reduction was carried out using the Pepi-AGE program (Dunkl et al., 2008), and the final statistical plotting was performed using Isoplot/Excel (Ludwig, 2003). The detailed procedures were described in Kawaguchi et al. (2021). In this study, $^{206}Pb/^{238}U$ dates are used for the zircon younger than 1000 Ma, while $^{207}Pb/^{206}Pb$ dates are used for the zircon older than 1000 Ma. Concordant dates were defined as the data points plotted on the Concordia curve within the 2σ error value. However, the data having a large discordance value (defined as the difference between $^{206}Pb/^{238}U$ and $^{207}Pb/^{235}U$ dates) of more than 10% was defined as the discordant dates.

Quality evaluation of pegmatite as source material for ceramic industry

All the quality evaluation tests of pegmatites for ceramic material were conducted at the Y My ceramic tile factory, Nhon Trach Industrial Park, Dong Nai Province, Vietnam. Pegmatite samples were ground to a fine powder using a mill with high alumina ceramic grinding balls. Powdered samples were dried using an oven under 100–105 °C and then added with a defined humidity of ~ 8 wt% before being compressed to form ~ 4 cm diameter circular specimens for calcination (1200 °C). Two standard samples FLC1 and FLC2 were used as reference materials for comparison, and they were prepared and processed in the same manner and conditions as the test samples. It should be noted that samples FLC1 and FLC2 are standard feldspars frequently used for ceramics manufacture at the Y My ceramic tile factory. To evaluate whether the studied pegmatites can be potentially used as a replacement of raw materials in ceramics manufacture, mixed samples SP1 and SP2 were also prepared, processed, and calcined under the same conditions as other test samples. Sample SP1 (49 wt% FLC1 mixed with 51 wt% other ingredients including kaolin, clay, and additives) is a product sample in the factory, and sample SP2 (49 wt% KT1907 mixed with 51 wt% same other ingredients as above) is the test sample used for quality comparison in this study. It is worth noting that samples SP1 and SP2 are the products of the unglazed tile categories (high-quality ceramic tile with water absorption of less than 0.5 wt%). All prepared samples including five test samples, two standards (FLC1 and FLC2), and two mixed samples (SP1 and SP2) were subsequently calcined under the same conditions in a roller kiln at a temperature of 1200 °C for a firing cycle of 38 min. After calcination, all the samples were evaluated for whiteness (%) (using a tristimulus colorimeter KangGuang SC-80), shrinkage rate (%) [based on the difference in diameter (mm) of test samples before and after calcination], loss on ignition (LOI; wt%), and water absorption rate (%) by comparing with standards and two samples in production considering the VN 6598:2000 standard (Science, 2000).

RESULTS

Whole-rock chemical compositions of pegmatites

Chemical compositions of major elements for collected samples and VN 6598:2000 standard are presented in Table 1. The SiO_2 contents range from 65.92 to 72.19 wt%, with an average value of 69.51 wt%, and are consistent with the silica content required for ceramic bone (Table 1). Most of the samples show a high content of Na_2O + K_2O ranging from 8.38 to 11.43 wt% and therefore are suitable for both ceramic bone and glaze (Table 1). Potassium dominates over sodium with the K_2O/Na_2O ratios ranging from 1.09 to 3.65 and thus classified as a potassic pegmatite (Norton and Redden, 1990). The Al_2O_3 content shows a moderate value of 14.81–16.13 wt%, whereas Fe_2O_3 is noticeably low (0.03–0.07 wt%).

LA-ICP-MS zircon U-Pb ages in the Kontum massif

The zircon U-Pb isotopic compositions and dates obtained from the LA-ICP-MS analysis are presented in Supplementary Table S1 (Supplementary Tables S1 is available online from https://doi.org/10.2465/jmps.210911). Cathodoluminescence images (CL) of representative zircon grains are shown in Figure 4, and concordia diagrams of the three studied pegmatites and three granitoids are presented in Figure 5.

First-stage pegmatite KT1903. Sixteen spots on sixteen zircon grains were selected for LA-ICP-MS analysis of which twelve spots were concordant. Zircon grains are light brown to colorless, transparent, mostly euhedral, and 50–120 μm in length with width-to-length ratios of approximately 1:2. The zircon grains show oscillatory zones in CL images (Fig. 4a). Th/U ratios of the concordant data predominantly range from 0.13 to 0.80. Two spots (spot numbers 076 and 084) showed younger concordant $^{206}Pb/^{238}U$ dates of 242–239 Ma (Fig. 4a). The main cluster of nine concordant analyses yielded a weight mean $^{206}Pb/^{238}U$ age of 448 ± 6 Ma (MSWD = 1.9) (Fig. 5a).

Two-mica granite KT1904 of the Ben Giang-Que Son Complex. Twenty spots on twenty zircon grains were selected for LA-ICP-MS analysis. The analyzed zircon grains are light brown to colorless, transparent, mostly euhedral, and 150–350 μm in length with width-to-length ratios of approximately 1:3. The zircon grains show oscillatory zones in CL images (Fig. 4b) and their Th/U ratios range from 0.13 to 2.33. Eighteen analyses yielded concordant dates and showed a weighted mean $^{206}Pb/^{238}U$ age of 240 ± 3 Ma, with a slightly high MSWD value of 2.5 (Fig. 5b). In addition, the weighted mean $^{206}Pb/^{238}U$ age of the youngest age cluster with overlapping dates under 2σ error (YC2σ) showed 236.9 ± 2.9 Ma (MSWD = 1.3, *n* = 13) (Fig. 5b).

Second-stage pegmatite KT1905. Twenty-three spots on twenty-three zircon grains were selected for LA-ICP-MS analysis of which seventeen spots are concordant. The analyzed zircon grains are light brown to colorless, transparent, mostly euhedral, and 100–200 μm in length with width-to-length ratios of approximately 1:2–1:3. The zircon grains show oscillatory zones in CL

Table 1. Major element and CIPW normative compositions of the studied pegmatites

Sample	VN1806	KT1907	KT1908	KT1909	KT1910	Average of 5 samples	Ceramic glaze*	Ceramic bone*
Latitude	14°02′09.1″N	14°28′42.3″N	14°29′18.9″N	14°29′51.3″N	14°29′57.6″N			
Longitude	108°31′54.7″E	108°12′05.2″E	108°13′05.6″E	108°14′13.8″E	108°14′12.7″E			
(wt%)								
SiO_2	69.95	68.70	70.79	72.19	65.92	69.51	≤ 70	≤ 75
TiO_2	0.14	0.06	0.06	0.05	0.06	0.07	≤ 0.02	-
Al_2O_3	16.13	15.16	14.96	14.81	15.05	15.22	≥ 16	≥ 14
Fe_2O_3	0.07	0.07	0.03	0.06	0.04	0.05	≤ 0.3	≤ 0.5
FeO	0.63	0.67	0.31	0.58	0.33	0.50		
MnO	0.00	0.10	0.01	0.02	0.01	0.03		
MgO	1.14	1.01	1.01	1.16	1.09	1.08		
CaO	0.62	1.08	0.95	1.23	1.01	0.98		
Na_2O	2.61	2.41	4.38	4.04	2.55	3.20		
K_2O	5.77	8.81	5.59	4.39	8.88	6.69		
P_2O_5	0.01	0.05	0.07	0.01	0.01	0.03		
LOI	2.94	1.88	1.84	1.45	5.05	2.63	≤ 0.5	≤ 0.5
K_2O+Na_2O	8.38	11.22	9.97	8.43	11.43	9.89	≥ 10	≥ 7
K_2O/Na_2O	2.21	3.65	1.28	1.09	3.48	2.34		
Q (CIPW)	30.18	17.15	20.75	27.50	14.17	21.95		
C	4.61	0.00	0.14	1.21	0.00	1.19		
Or	35.11	53.03	33.64	26.33	55.29	40.68		
Ab	22.75	20.78	37.76	34.68	22.73	27.74		
An	3.14	4.63	4.35	6.14	3.57	4.37		
Di (FS)	0.00	0.13	0.00	0.00	0.18	0.06		
Di (MS)	0.00	0.30	0.00	0.00	1.14	0.29		
Hy (MS)	2.93	2.43	2.56	2.93	2.33	2.64		
Hy (FS)	0.89	1.22	0.47	0.98	0.42	0.80		
Mt	0.10	0.11	0.05	0.09	0.06	0.08		
Il	0.27	0.11	0.11	0.10	0.12	0.14		
Ap	0.01	0.11	0.17	0.02	0.02	0.07		

LOI, loss on ignition.

* VN 6598:2000 standards with quality indices of raw materials for the ceramic production.

images (Fig. 4c) and their Th/U ratios mainly range between 0.19 and 0.46. One zircon grain (spot number 041) with a rounded shape gave an old $^{207}Pb/^{206}Pb$ concordant date of 1679 Ma, which indicates its xenocrystic origin. The main group of fourteen concordant spots yielded a weighted mean $^{206}Pb/^{238}U$ age of 269.4 ± 3.2 Ma (MSWD = 2.1) (Fig. 5c).

Third-stage pegmatite VN1806. Twenty-one spots on twenty zircon grains were selected for LA-ICP-MS analysis. Seventeen spots yielded concordant data. The analyzed zircon grains are light brown to colorless, transparent, mostly euhedral, and 100–250 µm in length with width-to-length ratios of approximately 1:2. The zircon grains used in the analysis show oscillatory zones in CL images (Fig. 4d) and their Th/U ratios range from 0.42 and 0.95. Seventeen concordant spots yielded a weighted mean $^{206}Pb/^{238}U$ age of 239 ± 3 Ma (MSWD = 1.4) (Fig. 5d).

Biotite granite KTM-Gr1802 of the Van Canh Complex. Twenty-eight spots on eighteen zircon grains were selected for U–Pb dating of which twenty-four spots were concordant. The analyzed zircon grains are colorless, transparent, mostly euhedral, and 100–150 µm length with width-to-length ratios of approximately 1:2 to 1:3. Most of the zircon grains have dark-oscillatory zoned cores and bright-weak oscillatory zoned or unzoned rims as observed in CL images (Fig. 4e). Th/U ratios of the concordant spots showed values between 0.26 and 0.91. Weighted mean $^{206}Pb/^{238}U$ ages of core and rim yielded 242.4 ± 2.6 Ma (MSWD = 1.4, n = 14) and 238.3 ± 3.1 Ma (MSWD = 0.94, n = 10), respectively, which indicate no significant age difference between them. Twenty-four concordant spots yielded a weighted mean $^{206}Pb/^{238}U$ age of 241.6 ± 1.7 Ma (MSWD = 1.09) with one rejected data (Fig. 5e).

Two-mica granite KTM-Gr1804 of the Van Canh Complex. Twenty-one spots on twenty-one zircon grains were dated, of which eighteen spots were concordant. The analyzed zircon grains are colorless, transparent,

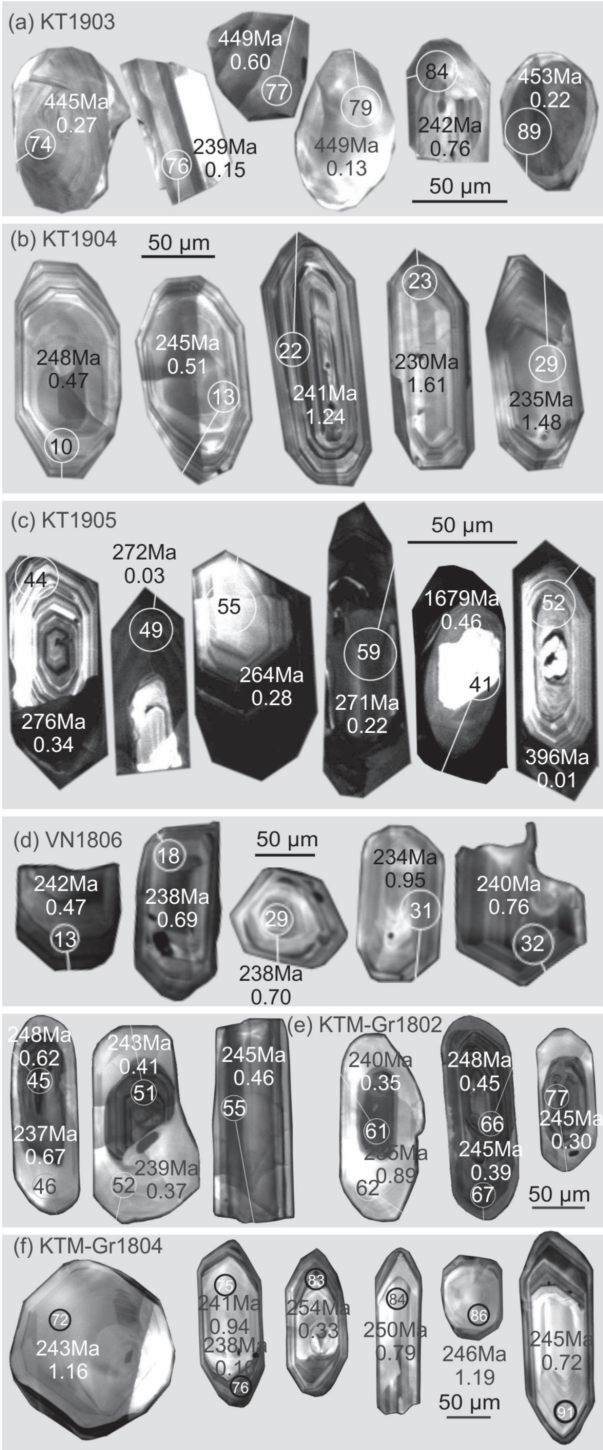

Figure 4. Cathodoluminescence images (CL) showing zircon textures from the pegmatites and granites. Each number inside the measurement spots represents the spot number corresponding to those in Supplementary Table S1. Concordant $^{206}Pb/^{238}U$ dates and Th/U ratio are also shown.

mostly euhedral, and show a length of 50–400 μm with width-to-length ratios of approximately 1:1 to 1:5. Most of the zircon grains show typical oscillatory zoning in the CL images (Fig. 4f). Th/U ratio of the concordant spots ranges from 0.1 to 1.34. Seventeen spots yielded a weighted mean $^{206}Pb/^{238}U$ age of 244.2 ± 3.2 Ma (MSWD = 1.6) (Fig. 5f).

Testing results for ceramic samples after calcination

After calcination, all the five test samples showed a higher shrinkage rate (5.2–11.1%) compared with the standard sample FLC2 (4.4%), especially samples KT1909 and KT1907 with distinctly high shrinkage rates of 10.0% and 11.1%, respectively (Table 2). The whiteness of test samples KT1910 and KT1905 were 88.65% and 83.5%, respectively, which are remarkably higher than that of standard samples FCL1 (74.2%) and FCL2 (81%) (Table 2). Test samples KT1909 and KT1907 showed the whiteness of 71.88% and 71.7%, respectively, slightly lower than that of the standard samples (Table 2). Only the sample, VN1806, displayed an abnormally dark brown color (Table 2 and Fig. 7a). For samples in production, all criteria indices of sample SP2 (replaced with 49 wt% raw material of sample KT1907) are similar to sample SP1 (using all ingredients from the factory) (Table 2).

DISCUSSION

Formation stages of pegmatites and granites

This study for the first time reports the age of the pegmatitic rocks in the Kontum massif by a more quantitative and high-resolution method of zircon U-Pb dating than the earlier works. Most of the analyzed zircon grains from three pegmatites and three host-rock granites show the oscillatory zoning under the CL image and yield Th/U ratios greater than 0.1. These criteria suggest that the studied zircon grains are of magmatic origin (Belousova et al., 2002; Hoskin and Schaltegger, 2003; Wu and Zheng, 2004).

LA-ICP-MS zircon U-Pb age dating of the first-stage pegmatite sample KT1903 showed a major cluster at the Ordovician period with a weighted mean age of ~ 448 Ma (Fig. 5a), representing the crystallization age of the pegmatite. The remaining spot age values of the other younger dates (242–239 Ma) might record the influence of a later-stage tectono-thermal activity probably due to the Pb-loss events as those dates were obtained mostly from the marginal part of zircon grains (Fig. 4a). In addition, surrounding areas of the first-stage pegmatite are occupied by the Permian-Triassic plutonic-metamorphic complexes, and our age dating results of zircon grains from host granite (KT1904) of the Ben Giang-Que Son Complex (~ 250–230 Ma; Fig. 5b) show a plausible correlation with the younger dates of the first-stage

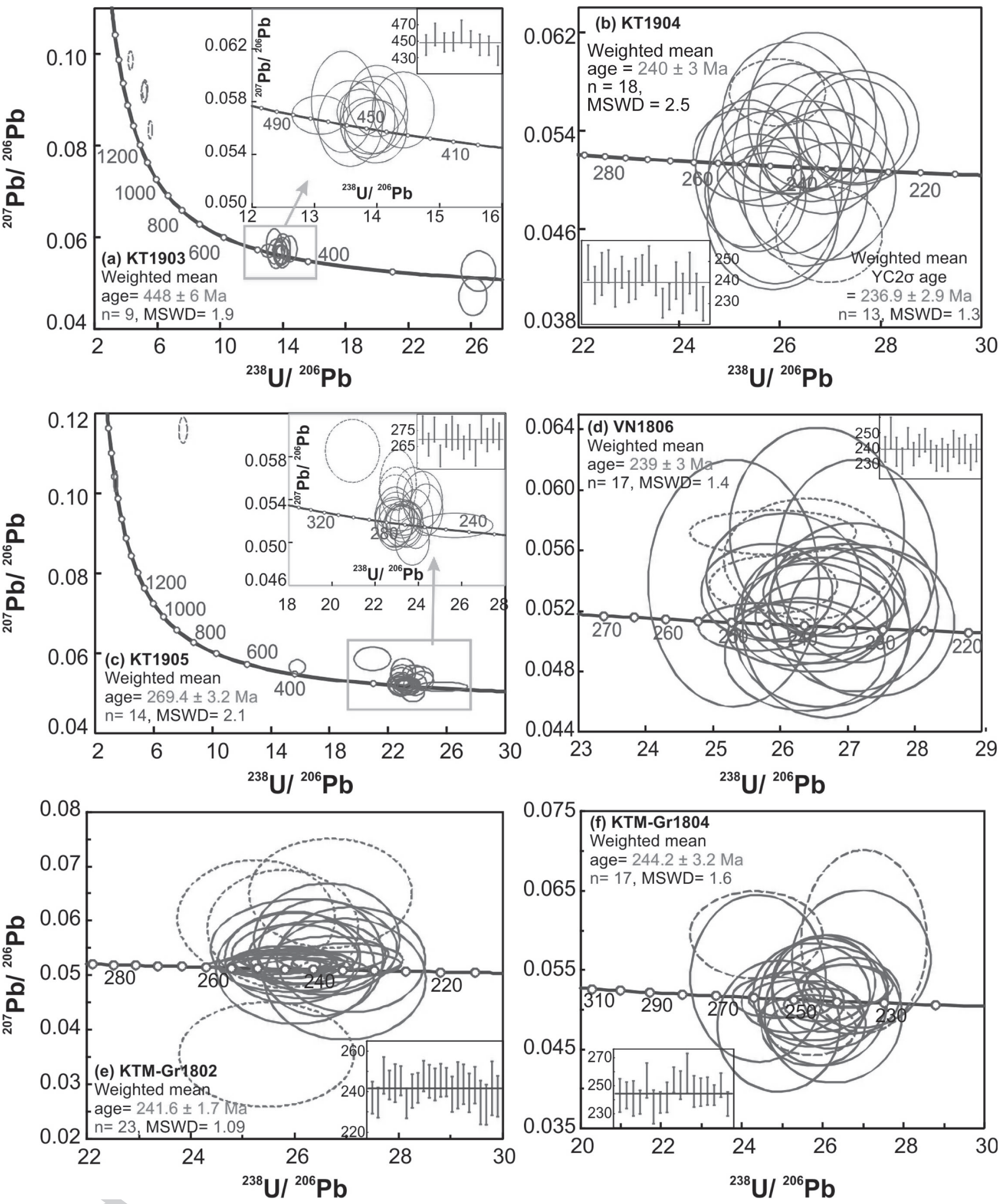

Figure 5. Concordia and weighted mean diagrams for zircon U-Pb dating results of the studied pegmatites and granites. Color version is available online from https://doi.org/10.2465/jmps.210911.

pegmatite (KT1903; Fig. 5a). The second-stage pegmatite (KT1905) yielded weighted mean age of ~ 269 Ma (Fig. 5c), representing the crystallization age of the pegmatites. The third-stage pegmatite (sample VN1806) showed a crystallization age of ~ 239 Ma (Fig. 5d). This age is temporally coincident with the widely distributed

Table 2. The quality indices of technological samples after calcination

No.	Sample	Shrinkage (%)	LOI (wt%)	Water absorption (%)	Whiteness (%)	Note
1	KT1910	6.8	0.5	14.6	88.65	Second-stage pegmatite, this study
2	KT1909	10.0	0.8	5.3	71.88	Second-stage pegmatite, this study
3	KT1907	11.1	0.6	3.3	71.7	Second-stage pegmatite, this study
4	KT1905	5.2	0.7	14.2	83.5	Second-stage pegmatite, this study
5	VN1806	11.0	0.8	2	Dark color	Third-stage pegmatite, this study
6	FLC1 (standard sample)	10.3	1.4	1.3	74.2	Pegmatite from Lao Cai
7	FLC2 (standard sample)	4.4	3.1	8.2	81	Pegmatite from Lao Cai
8	SP1 (sample in production at the factory)	10.3	8.1	<0.5	75.5	Sample in production at the factory
9	SP2 (sample in production at the factory)	10.2	7.9	<0.5	73	Replaced with 49% raw material of sample KT1907

LOI, loss on ignition.

magmatic suites in the study area (224–242 Ma; Hieu et al., 2015). With those, it is confirmed that the emplacement age of pegmatites in the Kontum massif spans three major phases: (1) the first-stage (sample KT1903) at 448 ± 6 Ma, (2) the second-stage (samples KT1905, KT1907, KT1909, and KT1910) at 269 ± 3.2 Ma, and (3) the third-stage (sample VN1806) at 239 ± 3 Ma.

Although the zircon grains with concordant dates from two-mica granite (KT1904) of the Ben Giang-Que Son Complex showed a single age cluster with a weighted mean age of 240 ± 3 Ma (MSWD = 2.5) (Fig. 5b), this age may not represent the crystallization age of granite due to its dispersed dates, which can be interpreted as a result of the existence of inherited/xenocrystic zircon grains. Instead, a weighted mean age of YC2σ (236.9 ± 2.9 Ma, MSWD = 1.3; Fig. 5b) is more appropriate to represent the crystallization age of the host granites to exclude the date of possible old inherited/xenocrystic zircon grains. Other two granites of the Van Canh Complex hosting the third-stage pegmatite (sample VN1806; 239 ± 3 Ma) show the intrusion ages of 244.2 ± 3.2 Ma and 241.6 ± 1.7 Ma (Figs. 5e and 5f). These ages indicate that the pegmatite was intruded shortly after the crystallization of the host granite basement and is likely the product of the final stage of magmatism generated from the host granites.

Magmatic-metamorphic activities generating pegmatites and their regional tectonic correlation around the Kontum massif

From the Late Ordovician period onwards, zircon crystals with oscillatory zoned parts of ~ 475–432 Ma (weighted mean $^{206}Pb/^{238}U$ age of 448 ± 6 Ma, sample KT1903; Fig. 5a) are showing the initial emplacement age of pegmatites. The obtained age is consistent with the Ordovician-Silurian magmatic-metamorphic activity (e.g., Hieu et al., 2016; Jiang et al., 2020; Minh et al., 2020; Trong et al., 2021). This timing can be presumably correlated with the closure of an ancient oceanic basin around the Kontum massif of the Indochina block (e.g., Tri and Khuc, 2011; Tran et al., 2014; Faure et al., 2018).

Late Permian and Early Triassic tectono-thermal events are recorded from a majority of analyzed zircon grains of pegmatites and host granites. These ages represent the most common magmatism or tectono-thermal stage resulting in extensive metamorphism in the Kontum massif (Fig. 6). Based on our field observations, these pegmatites occur in close association with the Ben Giang-Que Son Complex (KT1904; 236.9 ± 2.9 Ma, Fig. 5b). Several geological units and suture zones in Vietnam, such as the Tam Ky-Phuoc Son suture, the Song Ma suture, the Truong Son belt, and the Kontum massif, are reported to have been developed during the Permian-Triassic period (e.g., the Kan Nac Complex, 260–230 Ma) (Nam et al., 2001; Yan et al., 2006; Zhang et al., 2013; Hieu et al., 2017, 2019; Hung et al., 2021; Minh et al., 2021). Therefore, the Late Permian-Early Triassic ages of pegmatites and host granites can represent a significant tectonic phase that extensively triggered magmatism and metamorphism in the Indochina block and part of the South China block. It is convincing that this tectonic phase was temporally associated with the closure of the Paleo-Tethys along the Song Ma suture zone and the subsequent collision between the Indochina and South China blocks during the Permian-Triassic time, usually referred to as the Indosinian Orogeny (Hieu et al., 2019; Thanh et al., 2019).

Our age dating results are entirely consistent with most of the recent geological studies with zircon U-Pb ages in the Kontum massif suggesting that the area com-

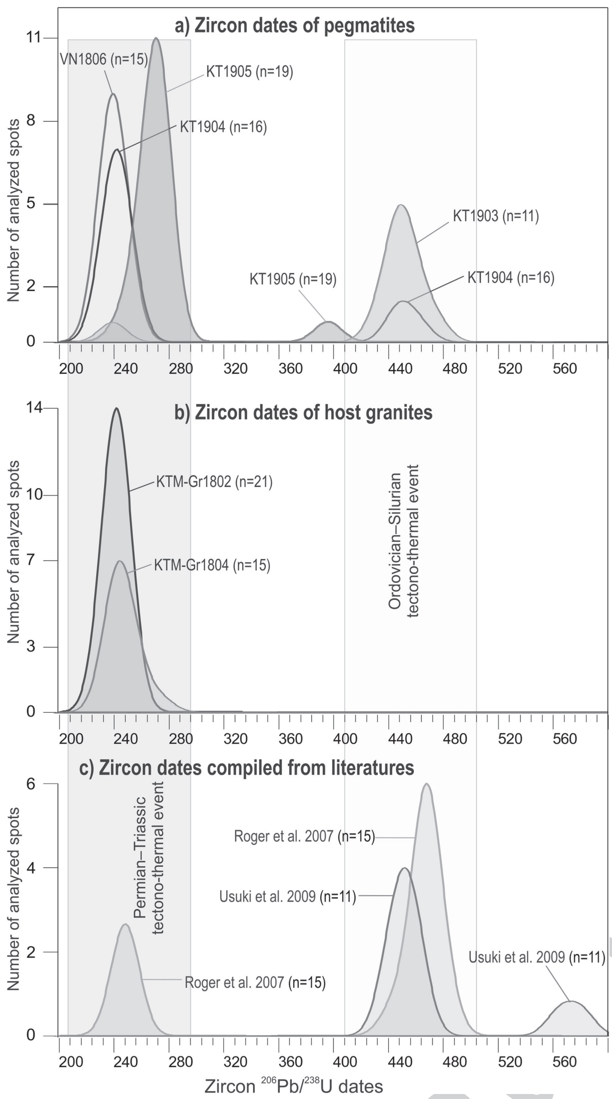

Figure 6. Probability density diagrams showing the magmatic-metamorphic stages recorded from zircon dates and their correlation with compiled data (Roger et al., 2007; Usuki et al., 2009) to establish major tectono-thermal events in the Kontum massif. Only the concordant data are used in constructing the plot. Color version is available online from https://doi.org/10.2465/jmps.210911.

prises two tectono-magmatic stages in the Phanerozoic, including the Ordovician-Silurian tectono-magmatic activities (Usuki et al., 2009; Hieu et al., 2016; Owada et al., 2016; Jiang et al., 2020; Minh et al., 2020; Nakano et al., 2021; Trong et al., 2021) and the Permian-Triassic magmatic-metamorphic activities (Nam et al., 2001; Hoa et al., 2008; Usuki et al., 2009; Sang, 2011; Nakano et al., 2021). The results of zircon U-Pb analyses in this study present a new finding on the emplacement ages of pegmatites, which is the Ordovician time, apart from the two well-known stages: Middle Permian and Middle Triassic periods in the Kontum massif (Fig. 6). Nevertheless, due to the complexity of the multi-stage geological evolution interpreted from currently limited data, more quantitative studies of pegmatites and related igneous activity are needed to acquire a comprehensive understanding of their evolutionary history and linkage with the surrounding rock bodies.

Potential application of the studied pegmatites in ceramic industry

Quality evaluation of the studied pegmatites for their potential application in ceramic materials plays an important role in the search and evaluation of pegmatite prospects to a broader extent in the territory of Vietnam. The testing results indicate that the second-stage pegmatites are the most prospective for further investigations and industrial applications. The first-stage pegmatite (KT1903) with noticeably high quartz content is not appropriate for calcined products, which was therefore not prepared for the quality evaluation and not recommended for ceramic materials.

As described above, the studied pegmatites show sufficient quality indices for total alkalinity with an overall high K_2O/Na_2O ratio, belonging to potassic pegmatite (Norton and Redden, 1990). In comparison to the Vietnam standard 6598:2000 for enamel, the total alkalinity and iron content, which affect the color after calcination, fulfill the standard criteria (Table 1). Although the Al_2O_3 content is slightly lower than the standard, it can be enriched by adding kaolinite. The loss on ignition is higher than the standard (Table 1) probably due to secondary alteration or the presence of primary hydrous minerals. Nevertheless, the loss on ignition generally does not affect the product quality.

The second-stage pegmatites after calcination were compared to the standard samples FLC1 and FLC2 (Fig. 7b) and show similar or higher whiteness (Table 2). Clumping of technological samples is evaluated based on the shrinkage rate after calcination (the higher the shrinkage, the better the clumping). Most of the test samples fall into the shrinkage range between standard samples FLC1 and FLC2, especially samples KT1909 and KT1907 with distinctly high shrinkage rates (Table 2), which indicate their sufficient clumping in ceramic manufacture. Most of the test samples (except for samples KT1910 and KT1905) show the water absorption value between the standard samples FLC1 and FLC2 (Table 2). They generally fulfill the criteria for water absorption.

For quality evaluation of the sample in production, sample SP2 (with 49 wt% substituting raw material of sample KT1907) after calcination shows the similar shrinkage, whiteness, and water absorption to those of sample SP1 (Table 2 and Fig. 7c). Therefore, it can be

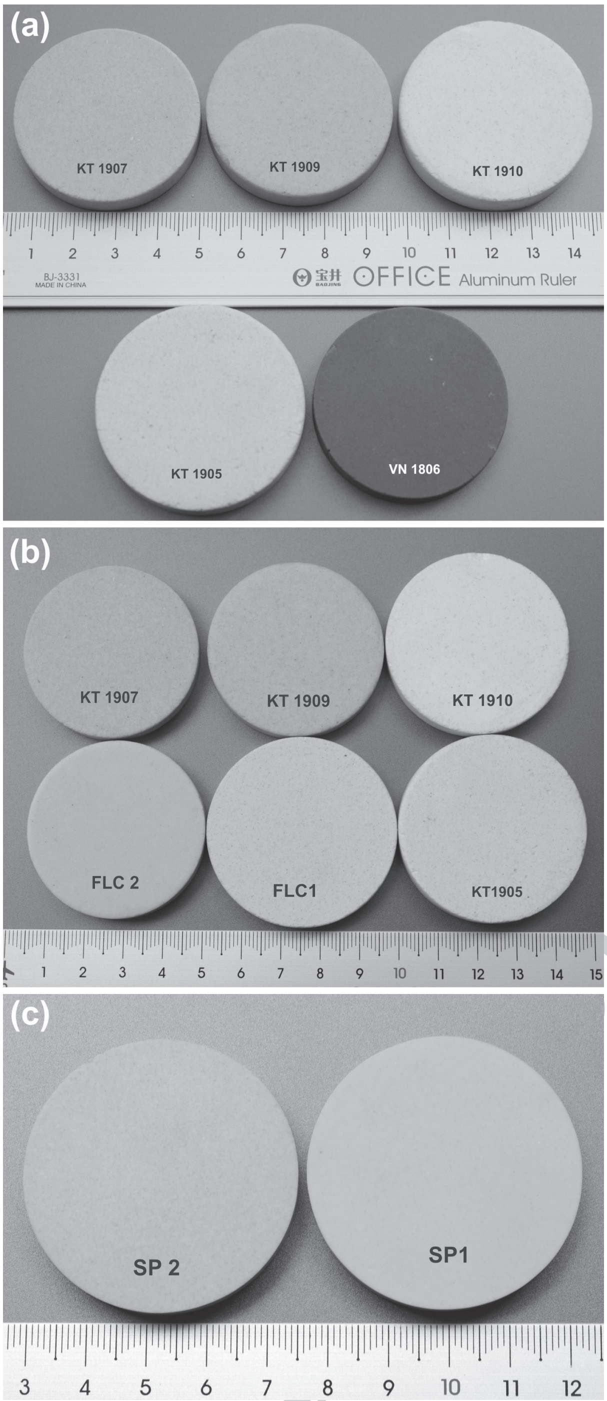

Figure 7. Technological samples after calcination: (a) Test samples, (b) Comparison of test samples and standard samples (FLC1 and FLC2), and (c) Comparison of samples in production at the factory (SP1 and SP2). Color version is available online from https://doi.org/10.2465/jmps.210911.

used as a sufficient quality material source for ceramic production.

The second-stage pegmatite (~ 269 Ma) will be an important replacement source for ceramic manufacture in the south of Vietnam in the future considering that most of the current factories producing ceramic tiles and household porcelain in southern Vietnam are using pegmatite materials from northern Vietnam (Phu Tho and Lao Cai Provinces) or imported from India and China. This finding guides the search, evaluation, and further exploration of pegmatite materials for the ceramic industry in Vietnam.

CONCLUSIONS

(1) This study for the first time reports the LA-ICP-MS zircon U-Pb ages of the pegmatitic rocks in the Kontum massif and confirmed the three separate timings of pegmatite formation: the first-stage at 448 ± 6 Ma, the second-stage at 269 ± 3.2 Ma, and the third-stage at 239 ± 3 Ma. Biotite-granite of the Ben Giang-Que Son Complex hosting first- and second-stage pegmatites showed the magmatic age of 236.9 ± 2.9 Ma. In addition, granites in the Van Canh Complex hosting the third-stage pegmatites showed the intrusion ages of 244.2 ± 3.2 Ma and 241.6 ± 1.7. Based on these ages, the third-stage pegmatite was intruded immediately after the emplacement of host granite. The first-stage pegmatite represents the late-magmatic product of the Ordovician-Silurian Period, associated with the closure of an ancient oceanic basin in central Vietnam. The second- and third-stage pegmatites together with granites of the Ben Giang-Que Son and Van Canh Complexes are likely related to the magmatism during Permian-Triassic collisional event between the South China and Indochina blocks.
(2) The second-stage pegmatites (~ 269 Ma) have chemical compositions and quality fulfilling the requirements for ceramic materials and are directly applicable in the ceramic industry in Vietnam.

ACKNOWLEDGMENTS

Thanks to Drs. T. Shibata and Y. Hayasaka of Hiroshima University for their assistance during the LA-ICP-MS zircon U-Pb dating. We further appreciate Ms. B.K. Ngoc of Vietnam National University, Ho Chi Minh City, and Mrs. H. Fujiwara and F. Sato of Hiroshima University for their support and discussion during the fieldwork. We express our gratitude to Dr. K. Das of Hiroshima University for his comments and check. Dr. T. Kawakami and an anonymous reviewer are highly appreciated for their constructive and insightful comments and Dr. M. Satish-Kumar for his handling and editorial comments. This research was funded by Vietnam National University Ho Chi Minh City (VNU-HCM) under grant number C2019-18-27. K.K. thankfully acknowledges the generous funding supported by the PEACE program of Hiroshima University.

SUPPLEMENTARY MATERIALS

Color version of Figures 1–3, 5–7 and Supplementary Table S1 are available online from https://doi.org/10.2465/jmps.210911.

REFERENCES

Bao, N.X. (2000) Tectonic and metallogenic map of southern Vietnam with the scale 1:1,000,000. Department of Geology and Mineral Resources Survey, Hanoi (In Vietnamese).

Belousova, E., Griffin, W.L., O'Reilly, S.Y. and Fisher, N. (2002) Igneous zircon: trace element composition as an indicator of source rock type. Contributions to Mineralogy Petrology, 143, 602–622.

Burnham, C.W. and Nekvasil, H. (1986) Equilibrium properties of granite pegmatite magmas. American Mineralogist, 71, 239–263.

Carter, A., Roques, D., Bristow, C. and Kinny, P. (2001) Understanding Mesozoic accretion in Southeast Asia: Significance of Triassic thermotectonism (Indosinian orogeny) in Vietnam. Geology, 29, 211–214.

Dunkl, I., Mikes, T., Simon, K. and von Eynatten, H. (2008) Brief introduction to the Windows program Pepita: data visualization, and reduction, outlier rejection, calculation of trace element ratios and concentrations from LA-ICP-MS data. In Laser ablation ICP-MS in the Earth Sciences: Current practices and outstanding issues (Sylvester, P. Ed.). Mineralogical Association of Canada Short Course, 40, 334–340.

Faure, M., Nguyen, V.V., Hoai, L.T.T. and Lepvrier, C. (2018) Early Paleozoic or Early-Middle Triassic collision between the South China and Indochina Blocks: The controversy resolved? Structural insights from the Kon Tum massif (Central Vietnam). Journal of Asian Earth Sciences, 166, 162–180.

Gramaccioli, C. and Segalstad, T. (1978) A uranium-and thorium-rich monazite from a south-alpine pegmatite at Piona, Italy. American Mineralogist, 63, 757–761.

Herzig, C.T., Kimbrough, D.L. and Hayasaka, Y. (1997) Early Permian zircon uranium-lead ages for plagiogranites in the Yakuno ophiolite, Asago district, Southwest Japan. The Island Arc, 6, 396–403.

Hieu, P.T. and Trung, H. (2015) U-Pb zircon age of quartz diorite from Ben Giang intrusive complex in the Ben Giang area, Quang Nam Province. Vietnam Journal of Earth Sciences, 37, 156–162 (In Vietnamese with English abstract).

Hieu, P.T., Yang, Y.-Z., Binh, D.Q., Nguyen, T.B.T., et al. (2015) Late Permian to Early Triassic crustal evolution of the Kontum massif, central Vietnam: zircon U-Pb ages and geochemical and Nd-Hf isotopic composition of the Hai Van granitoid complex. International Geology Review, 57, 1877–1888.

Hieu, P.T., Dung, N.T., Thuy, N.T.B., Minh, N.T. and Minh, P. (2016) U-Pb ages and Hf isotopic composition of zircon and bulk rock geochemistry of the Dai Loc granitoid complex in Kontum massif: Implications for early Paleozoic crustal evolution in Central Vietnam. Journal of Mineralogical and Petrological Sciences, 111, 326–336.

Hieu, P.T., Li, S.-Q., Yu, Y., Thanh, N.X., et al. (2017) Stages of late Paleozoic to early Mesozoic magmatism in the Song Ma belt, NW Vietnam: evidence from zircon U-Pb geochronology and Hf isotope composition. International Journal of Earth Sciences, 106, 855–874.

Hieu, P.T., Anh, N.T.Q., Minh, P. and Thuy, N.T.B. (2019) Geochemistry, zircon U-PB ages and HF isotopes of the Muong Luan granitoid pluton, Northwest Vietnam and its petrogenetic significance. Island Arc, 29, 12330.

Hoa, T.T., Anh, T.T., Phuong, N.T., Dung, P.T., et al. (2008) Permo-Triassic intermediate-felsic magmatism of the Truong Son belt, eastern margin of Indochina. Comptes Rendus Geoscience, 340, 112–126.

Hoskin, P.W.O. and Schaltegger, U. (2003) The composition of zircon and igneous and metamorphic petrogenesis. In Zircon (Hanchar, J.M. and Hoskin, P.W.O. Eds.). Reviews in Mineralogy and Geochemistry, 53, Mineralogical Society of America, Chantilly, VA, 27–62.

Hung, D.D., Tsutsumi, Y., Hieu, P.T., Minh, N.T., et al. (2021) Van Canh Triassic granite in the Kontum Massif, central Vietnam: geochemistry, geochronology, and tectonic implications. Journal of Asian Earth Sciences: X, 7, 100075.

Jiang, W., Yu, J.-H., Wang, X., Griffin, W., et al. (2020) Early Paleozoic magmatism in northern Kontum Massif, Central Vietnam: Insights into tectonic evolution of the eastern Indochina Block. Lithos, 376, 105750.

Kawaguchi, K., Minh, P., Hieu, P.T., Cuong, T.C. and Das, K. (2021) Evolution of supracrustal rocks of the Indochina Block: Evidence from new detrital zircon U-Pb ages of the Kontum Massif, Central Vietnam. Journal of Mineralogical Petrological Sciences, 116, 69–82.

Liu, F., Robinson, P.T., Gerdes, A., Xue, H., et al. (2010) Zircon U-Pb ages, REE concentrations and Hf isotope compositions of granitic leucosome and pegmatite from the north Sulu UHP terrane in China: constraints on the timing and nature of partial melting. Lithos, 117, 247–268.

London, D. (2021) Pegmatites, Encyclopedia of Geology, Second Edition. Academic Press, 184–195.

Ludwig, K.R. (2003) "User's manual for isoplot 3.00". Berkeley Geochronology Center Special Publication, 4, 1–71.

Mao, J., Du, A., Seltmann, R. and Yu, J. (2003) Re-Os ages for the Shameika porphyry Mo deposit and the Lipovy Log rare metal pegmatite, central Urals, Russia. Mineralium Deposita, 38, 251–257.

Minh, N.T., Dung, N.T., Hung, D.D., Minh, P., et al. (2020) Zircon U-Pb ages, geochemistry and isotopic characteristics of the Chu Lai granitic pluton in the Kontum massif, central Vietnam. Mineralogy and Petrology, 114, 289–303.

Minh, P., Hieu, P.T., Kawaguchi, K., Anh, N.T.Q. and Phuc, L.D. (2021) Geochemistry, zircon U-Pb geochronology and Sr-Nd-Hf isotopic composition of the Cha Val plutonic rocks in central Vietnam: Implications for Permian-Triassic Paleo-Tethys subduction-related magmatism. Vietnam Journal of Earth Sciences, 1–26.

Moore, P.B. (1971) Crystal chemistry of the alluaudite structure type: contribution to the paragenesis of pegmatite phosphate giant crystals. American Mineralogist, 56, 1955–1975.

Nagy, E.A., Maluski, H., Lepvrier, C., Schärer, U., et al. (2001) Geodynamic Significance of the Kontum Massif in Central Vietnam: Composite $^{40}Ar/^{39}Ar$ and U-Pb Ages from Paleozoic to Triassic. The Journal of Geology, 109, 755–770.

Nakano, N., Osanai, Y., Owada, M., Nam, T.N., et al. (2007) Geologic and metamorphic evolution of the basement complexes in the Kontum Massif, central Vietnam. Gondwana Research, 12, 438–453.

Nakano, N., Osanai, Y., Owada, M., Nam, T.N., et al. (2013) Tectonic evolution of high-grade metamorphic terranes in central Vietnam: constraints from large-scale monazite geochronology. Journal of Asian Earth Sciences, 73, 520–539.

Nakano, N., Osanai, Y., Owada, M., Binh, P., et al. (2021) Evolution of the Indochina Block from its formation to amalgamation with Asia: Constraints from protoliths in the Kontum Massif, Vietnam. Gondwana Research, 90, 47–62.

Nam, T.N., Sano, Y., Terada, K., Toriumi, M. and Van Quynh, P. (2001) First SHRIMP U–Pb zircon dating of granulites from the Kontum massif (Vietnam) and tectonothermal implications. Journal of Asian Earth Sciences, 19, 77–84.

Nguyen, Q.M., Feng, Q., Zi, J.-W., Zhao, T., et al. (2019) Cambrian intra-oceanic arc trondhjemite and tonalite in the Tam Ky–Phuoc Son Suture Zone, central Vietnam: Implications for the early Paleozoic assembly of the Indochina Block. Gondwana Research, 70, 151–170.

Norton, J.J. and Redden, J.A. (1990) Relations of zoned pegmatites to other pegmatites, granite, and metamorphic rocks in the southern Black Hills, South Dakota. American Mineralogist, 75, 631–655.

Osanai, Y., Nakano, N., Owada, M., Nam, T.N., et al. (2004) Permo-Triassic ultrahigh-temperature metamorphism in the Kontum massif, central Vietnam. Journal of Mineralogical and Petrological Sciences, 99, 225–241.

Owada, M., Osanai, Y., Nakano, N., Adachi, T., et al. (2016) Late Permian plume-related magmatism and tectonothermal events in the Kontum Massif, central Vietnam. Journal of Mineralogical and Petrological Sciences, 111, 181–195.

Paces, J.B. and Miller Jr, J.D. (1993) Precise U–Pb ages of Duluth complex and related mafic intrusions, northeastern Minnesota: Geochronological insights to physical, petrogenetic, paleomagnetic, and tectonomagmatic processes associated with the 1.1 Ga Midcontinent Rift System. Journal of Geophysical Research, 98, 13997–14013.

Roger, F., Maluski, H., Leyreloup, A., Lepvrier, C. and Truong Thi, P. (2007) U–Pb dating of high temperature metamorphic episodes in the Kon Tum Massif (Vietnam). Journal of Asian Earth Sciences, 30, 565–572.

Sang, Đ.Q. (2011) Petrographic characteristics and zircon U–Pb geochronology of granitoid rocks in the southern Bến Giằng, Quảng Nam province. Science & Technology Development, 14, 17–30 (in Vietnamese with English abstract).

Science, I.o.a.m. (2000) VN 6598:2000-Raw materials for construction ceramics – Feldspar, Vietnam Ministry of Construction, Publishing House, Hanoi, Vietnam.

Shi, M.-F., Lin, F.-C., Fan, W.-Y., Deng, Q., et al. (2015) Zircon U–Pb ages and geochemistry of granitoids in the Truong Son terrane, Vietnam: Tectonic and metallogenic implications. Journal of Asian Earth Sciences, 101, 101–120.

Thanh, T.V., Hieu, P.T., Minh, P., Nhuan, D.V. and Thuy, N.T.B. (2019) Late Permian–Triassic granitic rocks of Vietnam: the Muong Lat example. International Geology Review, 61, 1823–1841.

Thục, Đ.Đ., and Trung, H. (1995) Geology of Vietnam–Volume II: Magma Formations, pp. 359, Vietnam Geology Department (In Vietnamese).

Tinh, N.X., Pham, M., Do, N.T.H., Van Khoi, L. and Hieu, P.T. (2021) Zircon U–Pb isotope age and Hf isotope composition of the Ea H'leo granite in Dak Lak area. Science Technology Development Journal-Science of The Earth Environment, 5, 200–211 (in Vietnamese with English Abstract).

Tinh, T., Dung, L.T., Ty, N.H., Lich, N.V., et al. (1997) Geological and mineral map of Vietnam at scale 1:200 000 of the Mang Den–Bong Son sheet Geological survey and mineral of Viet Nam, Hanoi.

Toát, Đ.Đ. (2003) Research on evaluating the potential of feldspar as a ceramic material in Pegmatite, Kon Tum province. Hanoi University of Mining and Geology (in Vietnamese).

Tran, H.T., Zaw, K., Halpin, J.A., Manaka, T., et al. (2014) The Tam Ky–Phuoc Son Shear Zone in central Vietnam: Tectonic and metallogenic implications. Gondwana Research, 26, 144–164.

Tri, T.V. and Khuc, V. (2011) Geology and earth resources of Vietnam, Ha Noi, Vietnam, Publishing House for Science and Technology, pp. 634.

Trong, N.H., Zong, K., Liu, Y., Yuan, Y., et al. (2021) Early Paleozoic Arc Magmatism and Accretionary Orogenesis in the Indochina Block, Southeast Asia. The Journal of Geology, 129, 33–48.

Usuki, T., Lan, C.-Y., Yui, T.-F., Iizuka, Y., et al. (2009) Early Paleozoic medium-pressure metamorphism in central Vietnam: evidence from SHRIMP U–Pb zircon ages. Geosciences Journal, 13, 245–256.

Veksler, I.V. and Thomas, R. (2002) An experimental study of B-, P-and F-rich synthetic granite pegmatite at 0.1 and 0.2 GPa. Contributions to Mineralogy Petrology, 143, 673–683.

Wang, T., Tong, Y., Jahn, B.-m., Zou, T.-r., et al. (2007) SHRIMP U–Pb Zircon geochronology of the Altai No. 3 Pegmatite, NW China, and its implications for the origin and tectonic setting of the pegmatite. Ore Geology Reviews, 32, 325–336.

Wu, Y. and Zheng, Y. (2004) Genesis of zircon and its constraints on interpretation of U–Pb age. Chinese Science Bulletin, 49, 1554–1569.

Yan, D.-P., Zhou, M.-F., Wang, C.Y. and Xia, B. (2006) Structural and geochronological constraints on the tectonic evolution of the Dulong-Song Chay tectonic dome in Yunnan province, SW China. Journal of Asian Earth Sciences, 28, 332–353.

Zhang, R.Y., Lo, C.H., Chung, S.L., Grove, M., et al. (2013) Origin and Tectonic Implication of Ophiolite and Eclogite in the Song Ma Suture Zone between the South China and Indochina Blocks. Journal of Metamorphic Geology, 31, 49–62.

Manuscript received September 11, 2021
Manuscript accepted January 13, 2022

Manuscript handled by M. Satish-Kumar